Escape of about five per cent of Lyman-α photons from high-redshift star-forming galaxies

Matthew Hayes[1], Göran Östlin[2], Daniel Schaerer[1,3], J. Miguel Mas-Hesse[4], Claus Leitherer[5], Hakim Atek[6], Daniel Kunth[6], Anne Verhamme[7], Stéphane de Barros[1] & Jens Melinder[2]

[1]Observatoire Astronomique de l'Université de Genève, 51 chemin des Maillettes, CH-1290 Sauverny, Switzerland. [2]Oskar Klein Centre, Department of Astronomy, AlbaNova University Center, Stockholm University, 10691 Stockholm, Sweden. [3]Laboratoire d'Astrophysique de Toulouse-Tarbes, Université de Toulouse, CNRS, 14 Avenue E. Belin, 31400 Toulouse, France. [4]Centro de Astrobiología (CSIC-INTA), PO Box 78, 28691 Villanueva de la Cañada, Madrid, Spain. [5]Space Telescope Science Institute, 3700 San Martin Drive, Baltimore, Maryland 21218, USA. [6]Institut d'Astrophysique de Paris (IAP), 98bis boulevard Arago, 75014 Paris, France. [7]Oxford Astrophysics, Department of Physics, Denys Wilkinson Building, Keble Road, Oxford OX1 3RH, UK.

The Lyman-α (Lyα) emission line is the primary observational signature of star-forming galaxies at the highest redshifts[1], and has enabled the compilation of large samples of galaxies with which to study cosmic evolution[2–5]. The resonant nature of the line, however, means that Lyα photons scatter in the neutral interstellar medium of their host galaxies, and their sensitivity to absorption by interstellar dust may therefore be enhanced greatly. This implies that the Lyα luminosity may be significantly reduced, or even completely suppressed. Hitherto, no unbiased empirical test of the escaping fraction (f_{esc}) of Lyα photons has been performed at high redshifts. Here we report that the average f_{esc} from star-forming galaxies at redshift $z = 2.2$ is just 5 per cent by performing a blind narrowband survey in Lyα and Hα. This implies that numerous conclusions based on Lyα-selected samples will require upwards revision by an order of magnitude and we provide a benchmark for this revision. We demonstrate that almost 90 per cent of star-forming galaxies emit insufficient Lyα to be detected by standard selection criteria[2–5]. Both samples show an anti-correlation of f_{esc} with dust content, and we show that Lyα- and Hα-selection recovers populations that differ substantially in dust content and f_{esc}.

The hydrogen Lyα emission line, thanks to its high intrinsic luminosity ($L_{Ly\alpha}$)[1], high equivalent width ($W_{Ly\alpha}$)[6,7] and very convenient rest-frame wavelength (1,216 Å), continues to act as a staple tracer of distant star-forming galaxies. However, the Lyα transition is a resonant one, causing photons to scatter in the neutral hydrogen component (H I) of the interstellar medium, so that path lengths to escape may be greatly increased compared to non-resonant radiation. Thus, depending on the content, distribution and kinematics of H I, and the dust content, f_{esc} for a galaxy may fall anywhere within the range of 0 to 1 (refs 8–11). It follows that for the field of Lyα astrophysics to bloom—from using the line to select high-z galaxies, to a physically meaningful diagnostic of star formation—a detailed empirical examination of f_{esc} in cosmological galaxies is essential.

Estimating f_{esc} at high z is extremely challenging, because the requisite supporting data are observationally expensive to obtain. Comparison of star-formation rates (SFR) derived from Lyα with those from ultraviolet continuum can be used to infer $\langle f_{esc} \rangle$ = 30–60% from several studies of z = 2 and 3 Lyα samples[4,5,12]. However, this assumes that the ultraviolet continuum is un-attenuated, and is strongly dependent on models of stellar evolution to provide the respective SFR calibrations[13]. Furthermore, this technique is only valid if star formation has proceeded at a constant rate over the last ~100 Myr. More importantly, restricting analysis to Lyα-selected samples neglects potential star-forming galaxies that do not show Lyα emission. Comparing independently determined Lyα and ultraviolet luminosity functions provides an alternative, but cosmic variance can easily introduce errors of a factor of two (ref. 5), and the aforementioned uncertainties in SFR calibration remain. Using theoretical galaxy formation models, lower values of f_{esc} = 2% (ref. 14) to 10% (ref. 15) have been estimated at z = 3, but these methods suffer from the large number of *ad hoc* parameter assumptions that enter the models. A significant step forward can be taken if Lyα is compared with another, non-resonant hydrogen recombination line (for example, Hα), since both intrinsic strengths are a direct function of the ionizing luminosity. This has been done at z = 0.3, placing f_{esc} = 1–2% (ref. 16) but cosmological application is restricted by the >7 billion years over which galaxies can evolve to z > 2.

With a new, very deep survey using the ESO Very Large Telescope (VLT), we have overcome all of these issues simultaneously. We have performed a blind, unbiased, narrowband imaging survey for Hα and Lyα emission at $z = 2.2$ using custom manufactured filters to guarantee the same cosmic volume is probed in both emission lines (Supplementary Information). Thus, although cosmic variance does affect the number of objects in our survey volume, its effect cancels from any volumetric properties we derive by comparison of the two samples. With observational limits sensitive to un-obscured SFRs of 1.9 solar masses per year ($1.9 M_{\odot}$ yr^{-1}) in Hα, we identify 55 new Hα emitters[17]. Lyα observations are sensitive to SFR = $0.26 M_{\odot}$ yr^{-1} assuming $f_{esc} = 1$ ($f_{esc} = 0.13$ for the faintest Hα emitters), and we identify 38 new galaxies. Lyα and Hα luminosities are shown in Fig. 1 (see also Supplementary Information). Targeting the GOODS-South[18] field, we benefit from some of the deepest broadband optical and infrared data in existence, compiled into public source catalogues[19]. From these we obtain stellar spectral energy distributions (SEDs), which allow us to estimate dust content (E_{B-V}) and intrinsic SFR. We find all the Hα galaxies and 21 of the Lyα emitters in public catalogues.

From the Lyα sample we construct the observed Lyα luminosity function, LF(Lyα). Using the same formalism, we derive the first intrinsic Lyα luminosity function, LF(Lyα), from the Hα sample, using measurements of E_{B-V} to correct the Hα luminosity for extinction, and assuming the standard Lyα/Hα line ratio of 8.7 for ionization bounded nebulae[20] ("case B"; see Fig. 2). In this way, we obtain the intrinsic and observed Lyα luminosity densities, the ratio of which leads us directly to a volumetric $f_{esc} = (5.3 \pm 3.8)\%$, with no dependence on cosmic variance, the evolutionary state of the galaxies, or calibration uncertainties. The method is sensitive to the dust correction, as we assume that the same extinction applies to the continuum and to Hα, and thus we perform the same test without correcting Hα luminosities for dust, finding the most conservative upper limit of $(10.7 \pm 2.8)\%$ — a limit free of any model dependency whatsoever. This first key result shows that commonly practised survey estimates of the total Lyα luminosity density at $z \geq 2$ will significantly underestimate its intrinsic value: on average, only 1 in 20 of the intrinsic Lyα photons is accounted for. This may not be surprising at the highest redshifts (that is, above $z = 6$) where an

increase in the neutral fraction of the intergalactic medium may cause significant suppression of the Lyα line[21–23], but at z = 2–4 this effect is likely to be small, and the photons must be lost in the interstellar medium of individual galaxies. This result is especially consequential, because the integrated luminosity density converts directly to the cosmic rate of star-formation, implying that pure Lyα-based estimates of volumetric SFR are in need of strong upward revision.

To investigate the origin of this underestimate, we examine the individual galaxies. Having modelled the SEDs[24] for all the objects found in the broadband catalogues, we obtain homogeneous derivations of dust extinction (E_{B-V}) and SFR for both samples. From the Lyα and Hα luminosities, E_{B-V} estimates and recombination theory, we compute $f_{\rm esc}$ in individual sources (limits on $f_{\rm esc}$ are derived for sources detected in only one line by assigning the 1σ limiting flux to non-detections). In Fig. 3 we show how $f_{\rm esc}$ correlates with E_{B-V} for our observed galaxies, where we also plot the position of 50,000 synthetic galaxies generated using the 'MCLya' radiation transfer code[25], and the $f_{\rm esc}$–E_{B-V} relationship expected from pure dust attenuation[26]. All the synthetic galaxies fall below the theoretical curve, and every observed galaxy except for one lies within 1σ of this region. This demonstrates how Lyα photons are preferentially absorbed in the interstellar medium of almost all of our galaxies.

Despite the nonlinearity introduced by the multi-parametric Lyα transfer problem, $f_{\rm esc}$ and E_{B-V} remain clearly anti-correlated. The correlation shows a gradient that is 50% steeper than that predicted by pure dust attenuation: the effective extinction coefficient, k_{1216}, is found to be 17.8 instead of 12 for normal attenuation[26]. More striking in Fig. 3 is the lack of overlap and significant offset between the populations: the Lyα and Hα samples are almost disjoint in both quantities. We measure median values of E_{B-V} = 0.085 (0.23) and $f_{\rm esc}$ > 0.32 (<0.035) for Lyα (Hα) emitters. Furthermore, we find the median SFRs to be very different between the two samples: $3.5 M_{\odot}$ yr^{-1} for Lyα, and $10.0 M_{\odot}$ yr^{-1} for Hα. Thus Lyα galaxies are significantly less powerful in forming stars, less dusty, and show higher $f_{\rm esc}$ than Hα galaxies. For Lyα, these estimates are based on the 21 brighter galaxies found in public source catalogues and including the remainder would be likely to increase the disparity between the

samples. In f_{esc} the difference is further accentuated by the fact that we are considering lower and upper limits for the Lyα and Hα samples, respectively.

Another significant result is that of 55 Hα and 38 Lyα emitters, we detect only 6 galaxies in both lines. These galaxies straddle the individual distributions, with 5 of the 6 falling within 1σ of the dust attenuation curve. This is unsurprising when examined in light of the individual samples, but it is unlikely that such a relationship would have been predicted on the basis of the $z \approx 0$ objects of similar luminosity, where little obvious correlation is found between the two line intensities[8,27–29]. The fact that so few Hα emitters are detected in Lyα can be attributed to a combination of two factors. First, the extinction coefficient at Lyα is substantially larger than at Hα ($k_{1216} = 12.0$ compared to $k_{6563} = 3.33$)[26]: the median E_{B-V} for the Hα emitters corresponds to a 50% reduction in Hα luminosity but an f_{esc} value of just 7%. Second, the fact that only Lyα scatters serves to exacerbate this, and the grey points in Fig. 3 show how f_{esc} can be reduced to below 1%, even with minuscule dust contents. Indeed, for constant star formation (after the equilibrium time of ~100 Myr) with a 'standard' initial mass function and metallicity, $W_{Ly\alpha}$ is ~80 Å (refs 6, 7), and preferential suppression of Lyα by just a factor of 4 would render a galaxy undetected in the survey. Short-lived burst scenarios increase $W_{Ly\alpha}$ to >200 Å (refs 6, 7), requiring preferential attenuation factors of ~10; these are still easily attainable at very modest E_{B-V} (ref. 11). Similarly, the low number of Lyα sources detected in Hα is explained by the large range of escape fractions exhibited by star-forming galaxies: Lyα selection preferentially finds galaxies with higher f_{esc} values and smaller attenuation in Hα, resulting in line ratios nearer the recombination value and comparatively faint Hα. This pushes the Hα fluxes below our detection limit for most galaxies, despite the very deep Hα data.

Increasing the number of co-incident detections is extremely challenging observationally. Owing to the wide range of relative line intensities, a large range of luminosities needs to be spanned in both lines, requiring each observation to be both wide and deep. This is currently feasible in Lyα, but large (~0.5 degree^2) infrared imagers are still non-existent on telescopes of the 8–10-m class. Extending this survey to higher redshift will remain unfeasible until the James Webb Space Telescope comes online.

Received 28 September 2009; accepted 29 January 2010

References Cited

1. Partridge, R. B. & Peebles, P. J. E. Are young galaxies visible? Astrophys. J. **147,** 868–886 (1967).

2. Hu, E. M., Cowie, L. L. & McMahon, R. G. The density of Lya emitters at very high redshift. *Astrophys. J.* **502**, L99–L103 (1998).

3. Malhotra, S. & Rhoads, J. E. Large equivalent width Lya line emission at z=4.5: young galaxies in a young universe? *Astrophys. J.* **565**, L71–L74 (2002).

4. Gronwall, C. et al. Lya emission-line galaxies at z = 3.1 in the Extended Chandra Deep Field-South. *Astrophys. J.* **667**, 79–91 (2007).

5. Ouchi, M. et al. The Subaru/XMM-Newton Deep Survey (SXDS). IV. Evolution of Lya emitters from z=3.1 to 5.7 in the 1 deg2 field: luminosity functions and AGN. *Astrophys. J. Suppl. Ser.* **176**, 301–330 (2008).

6. Charlot, S. & Fall, S. M. Lyman-alpha emission from galaxies. *Astrophys. J.* **415**, 580–588 (1993).

7. Schaerer, D. The transition from Population III to normal galaxies: Lya and He ii emission and the ionising properties of high redshift starburst galaxies. *Astron. Astrophys.* **397**, 527–538 (2003).

8. Östlin, G. et al. The Lyman alpha morphology of local starburst galaxies: release of calibrated images. *Astron. J.* **138**, 923–940 (2009).

9. Atek, H. et al. Empirical estimate of Lya escape fraction in a statistical sample of Lya emitters. *Astron. Astrophys.* **506**, L1–L4 (2009).

10. Kornei, K. et al. The relationship between stellar populations and Lyman alpha emission in Lyman break galaxies. Preprint at ⟨http://arXiv.org/abs/0911.2000⟩ (2009).

11. Verhamme, A. et al. 3D Lya radiation transfer. III. Constraints on gas and stellar properties of z ~ 3 Lyman break galaxies (LBG) and implications for high-z LBGs and Lya emitters. *Astron. Astrophys.* **491**, 89–111 (2009).

12. Nilsson, K. K. et al. Evolution in the properties of Lyman-a emitters from redshifts z~3 to z~2. *Astron. Astrophys.* **498**, 13–23 (2009).

13. Kennicutt, R. C. Jr Star formation in galaxies along the Hubble sequence. *Annu. Rev. Astron. Astrophys.* **36**, 189–231 (1998).

14. Le Delliou, M., Lacey, C. G., Baugh, C. M. & Morris, S. L. The properties of Lya emitting galaxies in hierarchical galaxy formation models. *Mon. Not. R. Astron. Soc*. **365**, 712–726 (2006).

15. Nagamine, K., Ouchi, M., Springel, V. & Hernquist, L. Lyman-alpha emitters and Lyman-break galaxies at z=3–6 in cosmological SPH simulations. Preprint at ⟨http://arXiv.org/abs/0802.0228⟩ (2008).

16. Deharveng, J.-M. et al. Lya-emitting galaxies at 0.2<z<0.35 from GALEX spectroscopy. *Astrophys. J.* **680**, 1072–1082 (2008).

17. Hayes, M., Schaerer, D. & Östlin, G. The H-alpha luminosity function at redshift 2.2: a new determination using VLT/HAWK-I. *Astron. Astrophys.* **509**, L5–L9 (2010).

18. Giavalisco, M. et al. The Great Observatories Origins Deep Survey: initial results from optical and near-infrared imaging. *Astrophys. J.* **600**, L93–L98 (2004).

19. Santini, P. et al. Star formation and mass assembly in high redshift galaxies. *Astron. Astrophys*. **504**, 751–767 (2009).

20. Brocklehurst, M. Calculations of level populations for the low levels of hydrogenic ions in gaseous nebulae. *Mon. Not. R. Astron. Soc.* **153**, 471–490 (1971).

21. Santos, M. R. Probing reionization with Lyman a emission lines. *Mon. Not. R. Astron. Soc.* **349**, 1137–1152 (2004).

22. Dijkstra, M., Lidz, A. & Wyithe, J. S. B. The impact of the IGM on high-redshift Lya emission lines. *Mon. Not. R. Astron. Soc*. **377**, 1175–1186 (2007).

23. Hayes, M. & Östlin, G. On the narrowband detection properties of high-redshift Lyman-alpha emitters. *Astron. Astrophys.* **460**, 681–694 (2006).

24. Bolzonella, M., Miralles, J.-M. & Pelló, R. Photometric redshifts based on standard SED fitting procedures. *Astron. Astrophys.* **363**, 476–492 (2000).

25. Verhamme, A., Schaerer, D. & Maselli, A. III Lya radiation transfer. I. Understanding Lya line profile morphologies. *Astron. Astrophys*. **460**, 397–413 (2006).

26. Calzetti, D. et al. The dust content and opacity of actively star-forming galaxies. *Astrophys. J.* **533**, 682–695 (2000).

27. Giavalisco, M., Koratkar, A. & Calzetti, D. Obscuration of Ly alpha photons in star-forming galaxies. *Astrophys. J.* **466**, 831–839 (1996).

28. Atek, H., Kunth, D., Hayes, M., Östlin, G. & Mas-Hesse, J. M. On the detectability of Lya emission in star forming galaxies. The role of dust. *Astron. Astrophys.* **488**, 491–509 (2008).

29. Scarlata, C. et al. The effect of dust geometry on the Lya output of galaxies. *Astrophys. J*. **704**, L98–L102 (2009).

30. Isobe, T., Feigelson, E. D. & Nelson, P. I. Statistical methods for astronomical data with upper limits. II – Correlation and regression. *Astrophys. J*. **306**, 490–508 (1986).

Supplementary Information is linked to the online version of the paper at www.nature.com/nature.

Acknowledgements This work is based on observations made with ESO telescopes at the Paranal Observatory under programme ID 081.A-0932. The filter used to capture Lyα was financed by the Erik and Märta Holmberg foundation for astronomy and physics. M.H., D.S. and S.d.B. acknowledge the

support of the Swiss National Science Foundation. G.Ö. is a Swedish Royal Academy of Sciences research fellow supported by the Knut and Alice Wallenberg foundation, and also acknowledges support from the Swedish research council (VR). J.M.M.-H. is funded by Spanish MICINN grants CSD2006-00070 (CONSOLIDER GTC) and AYA2007-67965. We thank D. Valls-Gabaud, M. Ouchi, and C. Scarlata for discussions. M.H. thanks the people that made that Christmas at Cerro Paranal memorable.

Author Contributions M.H. and G.Ö. conceived the programme and manufactured the custom filter. M.H. observed, and processed and analysed the data. S.d.B. and D.S. wrote tools for analysis of the SED fitting results. A.V. produced the radiation transfer code with D.S. J.M. contributed to the use and processing of auxiliary data. All authors contributed to the interpretation of the data, the research proposal and manuscript preparation.

Author Information Reprints and permissions information is available at www.nature.com/reprints. The authors declare no competing financial interests. Correspondence and requests for materials should be addressed to M.H. (matthew.hayes@unige.ch).

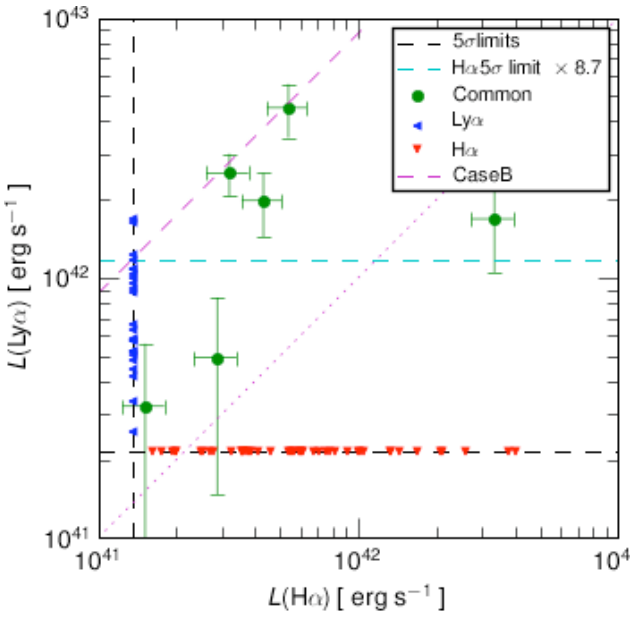

Figure 1. Observed Hα and Lyα luminosities. Sources detected only in Hα are shown in red, those detected only in Lyα in blue, and common detections in green. All error bars are 1σ photometric uncertainties. Objects undetected in Lyα or Hα are represented as upper limits placed at the detection limits of the Hα or Lyα data, respectively (black dashed lines). The dashed magenta line shows the Lyα/Hα ratio for case B recombination in the absence of dust, and the dotted line shows Lyα = Hα. For a

sample of dust-free galaxies, complete in both lines, all objects should line up on the recombination line, with dust and the effects of radiation transfer serving only to move objects away from the line in the direction of $L_{\mathrm{Ly}\alpha} < 8.7 L_{\mathrm{H}\alpha}$. The dashed cyan line shows 8.7 times the 5σ detection limit for Hα applied to the $L_{\mathrm{Ly}\alpha}$ axis. For the case B recombination ratio, all galaxies falling above this line should be detected in Hα (see Supplementary Information for more details). No objects occupy this region of the diagram with significance above 1σ.

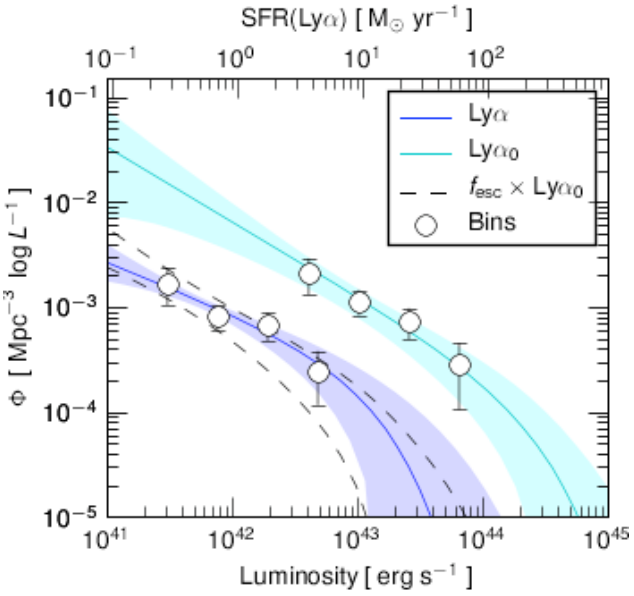

Figure 2. Lyα luminosity functions. Φ is the number density of galaxies per decade in luminosity. The SFR labelled on the upper abscissa corresponds directly to the luminosity on the lower. The luminosity function shaded blue, at lower luminosity, shows the observed luminosity distribution, derived from the VLT/FORS1 observations. The function shaded cyan, at higher luminosity, shows the intrinsic luminosity function, denoted LF(Lyα$_0$), derived from the HAWKI observations by correcting the Hα luminosities for dust attenuation, and multiplying by the case B Lyα/Hα ratio of 8.7. Black open circles show the bins of the respective luminosity functions, with vertical error bars representing 68% confidence limits. For the observed LF(Lyα), this error is derived from Poisson statistics and incompleteness simulations alone. For the intrinsic

LF(Lyα), the error bar also includes the error on the dust correction which is randomized on every realization of the Monte Carlo simulation, allowing galaxies to jump between adjacent bins (see Supplementary Information for details). The shaded regions associated with each luminosity function represent the regions of 68% confidence derived from the Monte Carlo. For each realization, both intrinsic and observed LF(Lyα) are regenerated and fitted with the Schechter function; integration over luminosity between 0 and infinity then provides us with the observed and intrinsic Lyα luminosity densities. Volumetric f_{esc} follows directly as the ratio of these two quantities, and is found to be (5.3 ± 3.8)%. Scaling the 68% limits of the intrinsic LF(Lyα) by this fraction in luminosity results in the dashed black lines, which clearly and comfortably encompass the observed distribution.

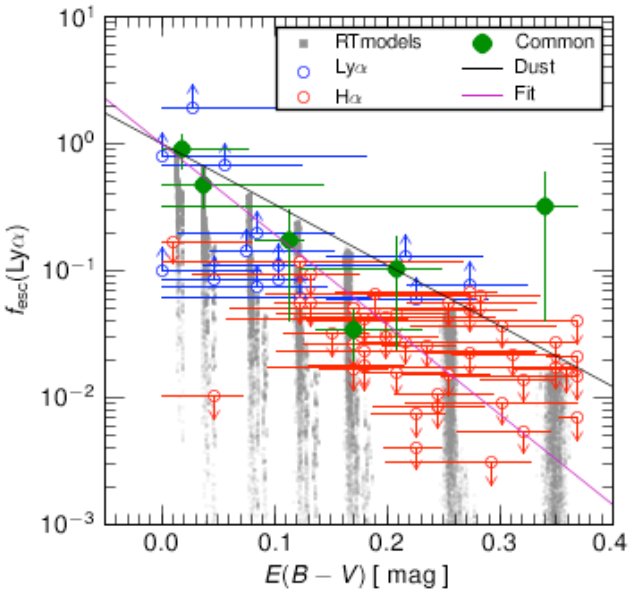

Figure 3. Escape fraction (f_{esc}) and dust attenuation (E_{B-V}). All objects found in the broadband photometry catalogue (that is, for which we can recover E_{B-V}) are included. Green shows galaxies detected in both lines, blue shows detections only in Lyα, and red shows detections only in Hα. All error bars are derived from propagation of measurement and model fit uncertainties, and represent 68% confidence. The grey clouds show the positions of 50,000 synthetic galaxies produced using the MCLya radiation transfer code, and are labelled R.T. models. The black line shows the dust

attenuation law of Calzetti, which should be valid in the absence of resonance scattering. The magenta line shows the relation that best fits the observed data points using Schmitt's binned linear regression algorithm[30], a survival analysis algorithm able to account for data points and limits in both directions which does not require a priori knowledge of the distribution of the censored parent population. The number of data points is 67 (55 Hα emitters + 18 Lyα emitters – 6 common detections). Parameterized as $f_{\rm esc} = 10^{-0.4 \times E_{B-V} \times k_{1216}}$, we find the extinction coefficient k_{1216} to be 50% higher (k_{1216} = 17.8 instead of 12.0) than the curve of pure dust attenuation. All but a few data points fall in the region swept out by the radiation transfer code, and demonstrate the significance of the spatial and kinematic structure of the neutral interstellar medium in the transfer of photons. Furthermore it is clear that the areas of the $f_{\rm esc}$–E_{B-V} diagram populated by Lyα- and Hα-selected galaxies are almost disjoint: the Lyα sample are significantly less dusty and exhibit higher escape fractions than the Hα sample. This clearly shows how the populations recovered by the respective selection functions are very different, despite the fact that the physics governing the production of the two emission lines is identical.